IEEE Access
Multidisciplinary ⋮ Rapid Review ⋮ Open Access Journal

Received 5 May 2024, accepted 14 May 2024, date of publication 21 May 2024, date of current version 31 May 2024.

Digital Object Identifier 10.1109/ACCESS.2024.3403861

RESEARCH ARTICLE

An Improved Z-Transform Finite Difference Time Domain Method for Electromagnetic Scattering and Plasma Stealth

CAIXIONG HAN[1], JIAJIE WANG[2], AND LANFANG DING[1]
[1]School of Mathematics and Physics, Qinghai University, Xining 810016, China
[2]School of Physics, Xidian University, Xi'an 710071, China

Corresponding author: Caixiong Han (hanqhu@163.com)

ABSTRACT The plasma sheath can absorb or reflect electromagnetic waves, thus affecting the communication of hypersonic vehicles. The study of attenuation and enhancement of electromagnetic scattering by plasma is of great significance. We propose a novel Z-transform finite-difference time-domain (ZT-FDTD) method to study the interaction between electromagnetic waves and plasmas. The numerical results show that this method has high accuracy and improves the computational efficiency by **9.8** percent, compared to the traditional ZT-FDTD method. We investigated the enhancement and attenuation of electromagnetic scattering by plasma at different plasma frequencies and plasma collision frequencies. The variation in the electric field amplitude in the plasma was studied under different electromagnetic scattering conditions. Through the hybrid plasma model, the changes in electromagnetic scattering and in the electric field amplitude under plasma stealth were further investigated. The position of the maximum electric field amplitude and the variation in the zero-value region of the electric field amplitude correspond to the different effects of plasma on electromagnetic scattering. The research methods and ideas in this study have important reference values and provide a new perspective for studying plasma stealth technology and solving the "blackout" problem.

INDEX TERMS Electromagnetic scattering, finite-difference time-domain (FDTD), plasma stealth, Z-transform.

I. INTRODUCTION

Hypersonic vehicles generate a plasma sheath upon re-entry into the atmosphere, which can absorb or reflect electromagnetic waves, thus impacting the communication of the vehicle and potentially causing communication disruptions. It is crucial to study the interaction between electromagnetic waves and plasma [1], [2]. The finite-difference time-domain (FDTD) methods applied to dispersive media, includes various numerical models such as the Recursive Convolution (RC) FDTD method [3], Auxiliary Differential Equation (ADE) FDTD method [4], Z-transform FDTD method [5], and Piecewise Linear Recursive Convolution (PLRC) FDTD method [6]. Chen uses the convolutional relationship between medium current density and electric field to derive the JE convolution (JEC) method for electromagnetic wave propagation in dispersive media [7]. The ZT-FDTD method has been used to analyze the reflection, attenuation, and scattering of electromagnetic waves in the plasma sheath [8], [9]. Yusuke et al. [10] demonstrated that the Drude model with plasma and collision frequencies can be used to characterize collisional plasmas. Liu et al. [11] analyzed the transmission characteristics of electromagnetic waves in various types of plasma using the finite-difference time-domain method. The scattering characteristics of electromagnetic waves in time-varying and non-uniform plasma sheaths were studied using the piecewise linear JE recursive convolution (PLJERC) finite-different time-domain (FDTD) method [12], [13]. Wang et al. utilized the Hybrid Implicit Explicit (HIE) - FDTD method to simulate rotational plasma in an open region [14]. A combined approach of Computational Fluid Dynamics (CFD) and finite-difference time-domain

The associate editor coordinating the review of this manuscript and approving it for publication was Mehmet Alper Uslu.

was employed to investigate the behavior of electromagnetic waves in plasma [10]. Plasma stealth technology is receiving increasing attention, both domestically and internationally. Yan et al. analyzed the effects of different electromagnetic wave frequencies and plasma collision frequencies on the plasma stealth effect using Z-FDTD [15].

Other numerical methods, such as the discontinuous Galerkin time domain (DGTD), Physical Optics (PO), and commercial software,have been widely used in the study of electromagnetic waves in plasma sheaths. Li et al. conducted a physical analysis of the interaction mechanism between a pulsed magnetic field and plasma flow field using COMSOL. [16]. Xu et al. introduced an exponential-based DGTD method to enhance the computational efficiency of the scattering characteristics of a hypersonic vehicle model surrounded by a uniform plasma layer [17]. Scarabosio et al. conducted a detailed analysis of the effects of the incident frequency, incident angle, and maximum plasma parameters on the electromagnetic scattering of three-dimensional plasma sheaths using physical optics (PO) methods [18]. Owing to the advantage of the FDTD method in terms of computational efficiency, the interaction between plasma and electromagnetic waves is mainly studied by FDTD [6], [8] combined with an effective dielectric constant model. In the study of plasma, the influence of detection environmental conditions such as lunar illumination intensity, lunar dust characteristics, and lunar ionospheric dust charging process on the amplitude and phase of electromagnetic waves was studied [19]. The envelope wave properties of a collisional non magnetized plasma model composed of cold ions, superheat electrons, and positive and negative dust particles was studied [20].

In this paper, we propose a novel ZT-FDTD method with high computational efficiency compared to the traditional method. This method has good accuracy and is easy for researchers familiar with ZT-transformation. To the best of our knowledge, this is the first time that this method has been developed for the FDTD method applied to dispersive media. The remainder of this paper is organized as follows. In Section II, formulations of the novel ZT-FDTD method are presented. In Section III, the accuracy of this method is confirmed by comparing it with the Mie theory, and the efficiency of this method is confirmed by comparing it with the conventional ZT-FDTD method. We studied the electromagnetic scattering and electric field amplitude under different plasma frequencies and plasma collision frequencies. Finally, conclusions are presented in Section IV.

II. ITERATIVE EQUATION OF ZT-FDTD

The dielectric coefficient is used to represent the characteristics of non magnetized media, and the frequency dependent dielectric coefficient can be expressed as follows:

$$\varepsilon(\omega) = \varepsilon_0[\varepsilon_\infty + \chi(\omega)] \tag{1}$$

where ε_∞ is the relative dielectric constant at infinity, ε_0 is the dielectric coefficient in vacuum, and χ_ω is the polarizability function.

A. DRUDE DISPERSIVE MEDIUM

The plasma sheath generated during the re-entry process of a hypersonic aircraft is usually considered cold plasma, which is expressed by a Drude dispersive medium [21]. In the Drude dispersive medium, χ_ω is given by

$$\chi(\omega) = -\frac{\omega_p^2}{\omega(\omega - j\upsilon_c)} \tag{2}$$

where ω_p is the plasma collision frequency and υ_c is the plasma frequency given by

$$\begin{aligned} \omega_p &= \sqrt{\frac{n_e e^2}{m_e \varepsilon_0}} \\ \upsilon_c &= n_s \sigma_{es} \sqrt{\frac{8\kappa T_v}{\pi m_e}} \end{aligned} \tag{3}$$

where m_e is the electron mass, n_e is the number density of electrons, n_s is the number density of species s, e is the magnitude of the electronic charge, and k is Boltzmann's constant. The effective electron-neutral energy exchange cross section is defined by a curve fit of the form.

$$\sigma_{es} = \widetilde{a_s} + \widetilde{b_s} T_e + \widetilde{c_s} T_e^2$$

The constants for Eq.(3) are presented in Table. 1 [21].

TABLE 1. Constants for curve fits of electron-neutral energy exchange cross section, σ_{es}.

s	$\tilde{a_s}$	$\tilde{b_s}$	$\tilde{c_s}$
N	5E-20	0	0
O	1.2E-20	1.7E-24	-2E-29
N_2	7.5E-20	5.5E-24	-1E-28
O_2	2E-20	6E-24	0
NO	1E-19	0	0

B. THE TRADITIONAL Z-TRANSFORM FDTD METHOD

The Maxwell expressions are:

$$\begin{aligned} \nabla \times E &= -\frac{\partial B}{\partial t} - \sigma_m H \\ \nabla \times H &= \frac{\partial D}{\partial t} + \sigma E \\ B &= \mu H \\ D(\omega) &= \varepsilon(\omega) E(\omega) \end{aligned} \tag{4}$$

Substituting Eq.(1) and Eq.(2) into Eq.(4), we obtain

$$\tilde{D}(\omega) = \varepsilon(\omega)\tilde{E}(\omega) = \varepsilon_0(\varepsilon_\infty + \frac{\sigma}{j\omega\varepsilon_0} + \frac{\omega_p^2}{\omega(j\upsilon_c - \omega)})\tilde{E}(\omega) \tag{5}$$

where, σ is electrical conductivity.

$$\varepsilon(\omega)=\varepsilon_0(1+\frac{\omega_p^2}{\omega(j\nu_c-\omega)})=\varepsilon_0(1+\frac{\omega_p^2/\nu_c}{j\omega}-\frac{\omega_p^2/\nu_c}{j\omega+\nu_c}) \quad (6)$$

Perform Z-transform on Eq.(6)

$$\varepsilon(z)=\frac{1}{\Delta t}+\frac{\omega_p^2/\nu_c}{1-z^{-1}}-\frac{\omega_p^2/\nu_c}{1-\exp(-\nu_c\Delta t)z^{-1}} \quad (7)$$

Introducing auxiliary variables **I** and **S**

$$\begin{aligned} I(z)&=\frac{\Delta t\omega_p^2/\nu_c}{1-z^{-1}}E(z)\\ &=z^{-1}I(z)+\frac{\omega_p^2\Delta t}{\nu_c}E(z) \end{aligned} \quad (8)$$

$$\begin{aligned} S(z)&=-\frac{-\Delta t\omega_p^2/\nu_c}{1-z^{-1}\exp(-\nu_c\Delta t)}E(z)\\ &=\exp(-\nu_c\Delta t)z^{-1}S(z)-\frac{\Delta t\omega_p^2}{\nu_c}E(z) \end{aligned} \quad (9)$$

We can get the z-domain $D(z)$,

$$\begin{aligned} D(z)&=\varepsilon_0[\varepsilon_\infty E(z)+I(z)+S(z)]\pi\\ &=\varepsilon_0\varepsilon_\infty E(z)+\varepsilon_0 z^{-1}I(z)+\frac{\varepsilon_0\omega_p^2\Delta t}{\nu_c}E(z)\\ &\quad+\varepsilon_0\exp(-\nu_c\Delta t)z^{-1}S(z)-\frac{\varepsilon_0\Delta t\omega_p^2}{\nu_c}E(z)\\ &=\left[\varepsilon_0\varepsilon_\infty+\frac{\varepsilon_0\omega_p^2\Delta t}{\nu_c}+-\frac{\varepsilon_0\Delta t\omega_p^2}{\nu_c}\right]E(z)\\ &\quad+\varepsilon_0 z^{-1}I(z)+\varepsilon_0\exp(-\nu_c\Delta t)z^{-1}S(z)\\ &=\varepsilon_0\varepsilon_\infty E(z)+\varepsilon_0 z^{-1}I(z)+\varepsilon_0\exp(-\nu_c\Delta t)z^{-1}S(z) \end{aligned} \quad (10)$$

So, $E(z)$ is

$$E(z)=\frac{D(z)-\varepsilon_0 z^{-1}I(z)-\varepsilon_0\exp(-\nu_c\Delta t)z^{-1}S(z)}{\varepsilon_0\varepsilon_\infty} \quad (11)$$

C. THE NOVEL Z-TRANSFORM FDTD METHOD

In the novel ZT-FDTD method, perform Fourier transform on Eq.(4), we obtain

$$\begin{aligned} F(\varepsilon\frac{\partial E(t)}{\partial t})&=\varepsilon(\omega)\cdot j\omega E(\omega)\\ &=\varepsilon_0(1+\frac{\omega_p^2}{\omega(j\nu_c-\omega)})\cdot j\omega E(\omega)\\ &=j\omega\varepsilon_0 E(\omega)+\frac{\omega_p^2\varepsilon_0}{\nu_c+j\omega}E(\omega)\\ &=j\omega\varepsilon_0 E(\omega)+J(\omega) \end{aligned} \quad (12)$$

where,

$$J(\omega)=\frac{\omega_p^2\varepsilon_0}{\nu_c+j\omega}E(\omega) \quad (13)$$

Perform Z-transform on Eq.(13)

$$J(z)(\nu_c+\frac{1\text{-}z^{-1}}{z^{-1}\Delta t})=\omega_p^2\varepsilon_0 E(z) \quad (14)$$

Perform $z^{-1}J_p(z)\rightarrow {J_p}^{n-1}$ on above formula, we can gain

$$\begin{aligned} J(t)^n&=(1\text{-}\nu_c\Delta t)J(t)^{n-1}+\omega_p^2\varepsilon_0\Delta t\cdot E(t)^{n-1}\\ E(t)^n&=\frac{\Delta t}{\varepsilon_0}(\nabla\times H-J(t)^n)+E(t)^{n\text{-}1} \end{aligned} \quad (15)$$

The above formula is the Z-transform method for dispersive media.The propagation of electromagnetic waves in dispersive media can be calculated using Eq.(4) and Eq.(15). The time-domain stepping steps are summarized as follows

1) $\mathbf{E}\longrightarrow\mathbf{J_p}$,
2) $\mathbf{E}\longrightarrow\mathbf{H}$,
3) $(\mathbf{J_p},\mathbf{H})\longrightarrow\mathbf{E}$.

In the traditional ZT-FDTD method, the iterative formula introduces auxiliary variables **D**, **I**, and **S**, and thus,consumes more memory. We propose a novel Z-transform FDTD method that introduces intermediate variable **S** and simplifies the formulas. Assuming that the incident wave is polarized along the x-direction, the complex amplitude of the electric magnetic field are

$$\begin{aligned} E_i&=e_x E_{im}e^{-jk_1z}\\ H_i&=e_y\frac{E_{im}}{Z_c}e^{-jk_1z} \end{aligned} \quad (16)$$

The complex amplitude of the electric and magnetic field of the reflected wave are

$$\begin{aligned} E_r&=e_x RE_{im}e^{jk_1z}\\ H_r&=-e_y\frac{RE_{im}}{Z_c}e^{-jk_1z} \end{aligned} \quad (17)$$

The reflection coefficient is

$$R=\frac{Z_{c2}-Z_{c1}}{Z_{c2}+Z_{c1}} \quad (18)$$

where, subscripts 1 and 2 represent medium 1 and medium 2.

To obtain the scattering outside the calculated region, it is necessary to build a closed surface in the calculated region according to the equivalence principle, and then extrapolate the equivalent electromagnetic current on the surface to obtain the scattering. Monostatic RCS [22] can be represented by the scattering field equation given

$$RCS(f)=10\lg(4\pi r^2\left|\frac{E_x(f)}{E_i(f)}\right|^2) \quad (19)$$

where, f is the incident wave frequency, E_x is the far-field, and E_i is the incident wave.

III. EXAMPLES

Three numerical experiments are conducted to verify the effectiveness of the novel Z-transform FDTD.

A. REFLECTION COEFFICIENT FOR A PLASMA SLAB

To verify the reliability of the numerical method, the reflection coefficient of the plasma flat plate on electromagnetic waves was calculated. The thickness of the flat plate is 0.015 m, the incident wave is a Gaussian pulse, the spatial step size is 75 um, the plasma frequency and the collision frequency are $\omega_p = 2\pi \times 28.7 \times 10^9 rad/s$, $\upsilon_c = 2.0 \times 10^{10} Hz$, the number of iteration is 12000.

Figure 1 shows the calculation of the reflection coefficient of electromagnetic waves passing through a plasma plate using the analytical method, improved ZT-FDTD, traditional ZT-FDTD, PLRC-FDTD, and SO-FDTD methods, and shows the memory and operating time consumed by each method.

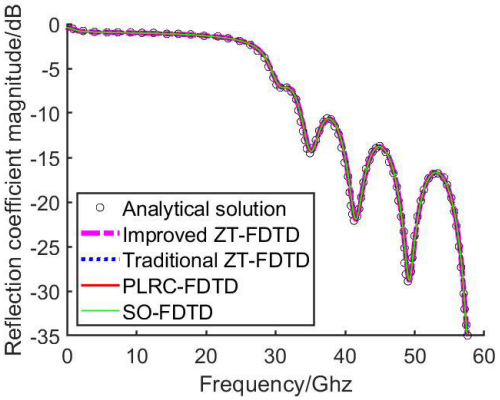

FIGURE 1. Monostatic RCS of the Plasma Sphere.

As shown in Table. 2, the new method required only **90.26** percent of the time of the traditional ZT-FDTD method and consumes the least amount of memory. PLRC-FDTD method takes the most running time, and SO-FDTD method consumes the most memory.

TABLE 2. Comparison of running time cost and memory consumption.

Numerical Methods	CPU time (s)	RAM(Mb)
Improved ZT-FDTD	288.8182	2491.76
Traditional ZT-FDTD	319.9635	2540.78
PLRC-FDTD	416.2716	2491.42
SO-FDTD	319.4827	2558.42

B. RCS OF A PLASMA SPHERE

we calculate the monostatic radar cross section (RCS) of a plasma ball ($\omega_p = 2\pi \times 28.7 \times 10^9 rad/s, \upsilon_c = 2.0 \times 10^{10} Hz, r = 3.5mm$). The incident wave is a Gaussian pulse, Yee-cell step size $\delta = 0.0875mm$, the number of iteration is 5400.

As shown in Figure 2, a very good agreement is achieved among the results obtained using the novel Z-transform FDTD method and the Mie theory. As shown in table. 3, when the incident wave frequency is around 4 GHz, RCS error is small. When the incident wave frequency is around 8 GHz, RCS error is significant. This is mainly because as the

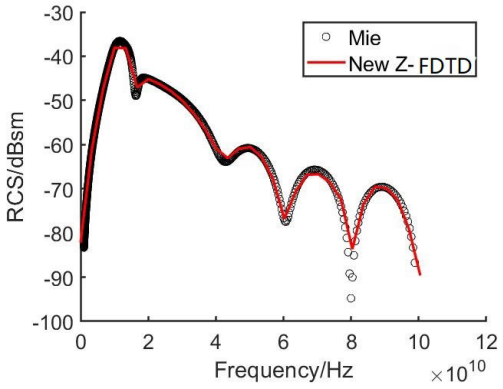

FIGURE 2. Monostatic RCS of the Plasma Sphere.

TABLE 3. RCS error.

Frequency	6.01(GHz)	8.0(GHz)	10.0(GHz)
RCS error	0.53dBsm	13.08dBsm	2.08dBsm

frequency increases, the size of wavelength dispersion decreases.

C. RCS OF INHOMOGENEOUS PLASMA FLOW AROUND BLUNT CONE

Next, we calculated the bistatic RCS of a metal sphere covered by uniform plasma. As shown in Figure 3, $r_1 = 0.04m$, $r_2 = 0.07m$, the radius of the metal ball is r_1, the slab of plasma is $d = r_2 - r_1 = 0.03m$, the plane wave has a wavelength of $\lambda = 0.08m$, Yee-cell step size $\delta = \lambda/40$. The influence of six types of plasma on electromagnetic scattering was studied experimentally, and their parameters are listed in Table. 4.

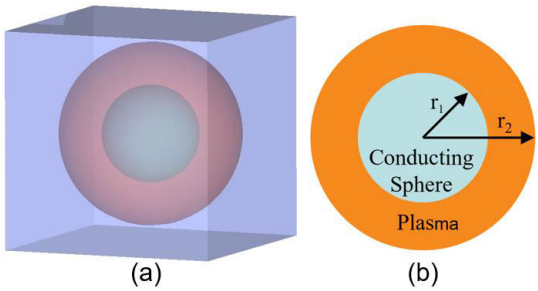

FIGURE 3. (a) 3D Model, (b) Model sizes.

TABLE 4. Plasma parameters.

Medium	$\omega_p\,(rad/s)$	$\upsilon_c\,(Hz)$
Plasma 1	40.0×10^9	1.0×10^9
Plasma 2	60.0×10^9	1.0×10^9
Plasma 3	80.0×10^9	1.0×10^9
Plasma 4	40.0×10^9	50.0×10^9
Plasma 5	40.0×10^9	60.0×10^9
Plasma 6	40.0×10^9	80.0×10^9

In theory, when the plasma frequency is greater than the incident wave frequency, the smaller the incident wave

frequency, the more difficult it is to pass through the plasma and the more obvious the reflection [2]. At this point, the plasma enhances electromagnetic scattering.

As shown in Figure 4, two conductor spheres with radius r_1 and r_2. The plasma collision frequency is 1GHz, and the plasma frequencies of plasma 1, plasma 2, and plasma 3 are $40.0 \times 10^9 rad/s$, $60.0 \times 10^9 rad/s$ and $80.0 \times 10^9 rad/s$ respectively. When the plasma collision frequency is constant, the higher the plasma frequency, the larger is the RCS.

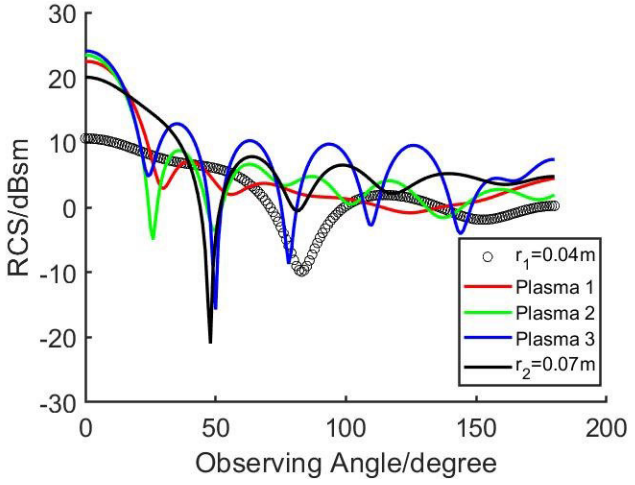

FIGURE 4. Bistatic RCS of the Conducting Sphere with plasma 1, plasma 2 and plasma 3 obtained by the new Z-FDTD method.

As shown in Figure 5 (a), the electric field amplitude in the conductor sphere region is zero. As shown in Figure 5 (b), (c), and (d), as the plasma frequency increased, the zero region of the electric field amplitude in the plasma increased. When the plasma frequency increased to a certain limit, the impact of the plasma on the RCS approached that of a conductor.

As shown in Figure 6, the plasma frequency is $40.0 \times 10^9 rad/s$, and the plasma collision frequencies are $50GHz$, $60GHz$ and $80GHz$. Owing to the collision absorption of plasma, electromagnetic waves are greatly attenuated in the plasma. As the collision frequency of the plasma increases, becomes smaller the RCS, becomes more obvious the plasma stealth effect.

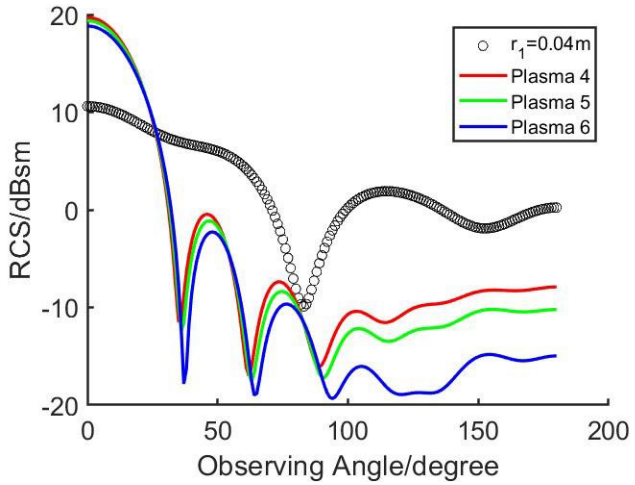

FIGURE 6. Bistatic RCS of the Conducting Sphere with plasma 4, plasma 5 and plasma 6 obtained by the new Z-FDTD method.

As shown in Figure 7 (b), (c), and (d), as the collision frequency of the plasma increases, the variation in the electric field in the plasma gradually decreased, and the maximum

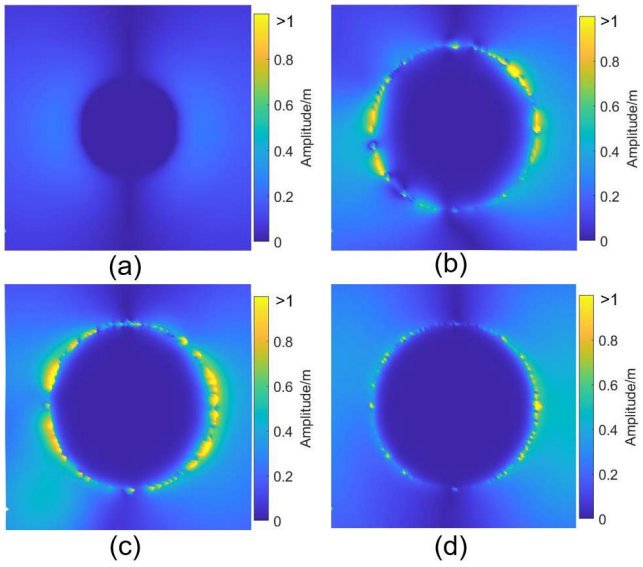

FIGURE 5. (a) electric field amplitude of conducting sphere, (b) electric field amplitude of conducting sphere with plasma 1, (c) electric field amplitude of conducting sphere with plasma 2, (d) electric field amplitude of conducting sphere with plasma 3.

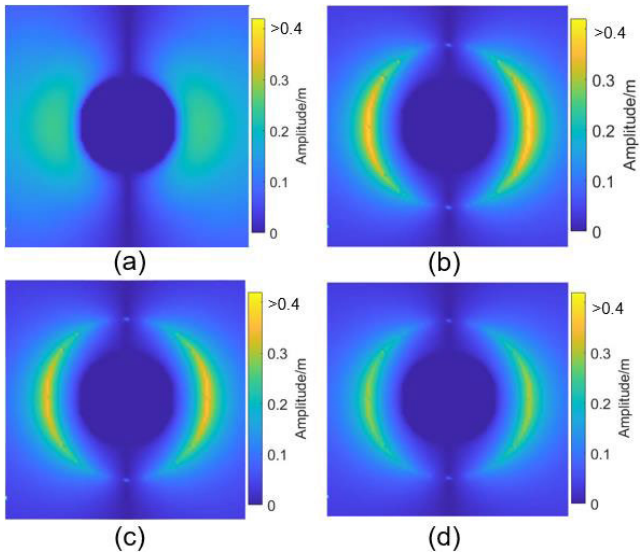

FIGURE 7. (a) electric field amplitude of conducting sphere, (b) electric field amplitude of conducting sphere with plasma 4, (c) electric field amplitude of conducting sphere with plasma 5, (d) electric field amplitude of conducting sphere with plasma 6.

value of the electric field amplitude was located at the outer edge of the plasma.

Based on the above conclusions, we can see that plasma 1, plasma 2, and plasma 3 have an increasing effect on RCS, while plasma 4, plasma 5, and plasma 6 have a decreasing effect on RCS. Next, we will study the impact of hybrid plasma on RCS. In the plasma sheath generated around a reentry vehicle, the inner plasma layer contributes to an increase in RCS, while the outer plasma layer attenuates the RCS. On the basis of the original plasma region 1 (as shown in Figure 8), we add a region 2 with a thickness of d filled with plasma 4, plasma 5, and plasma 6.

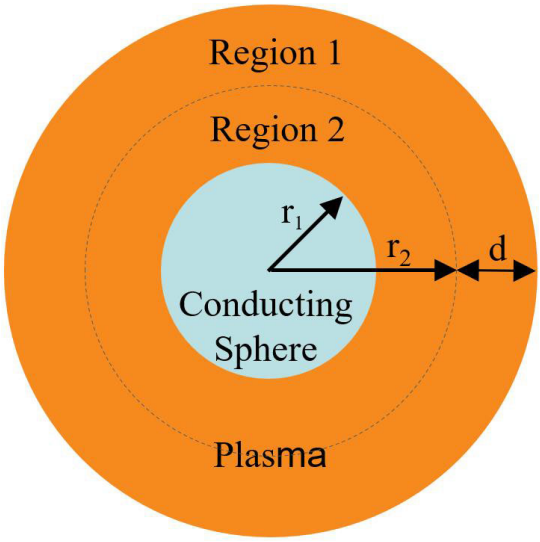

FIGURE 8. Hybrid plasma model.

As shown in Figure 9, we filled plasma1 in region 1, and plasma4, plasma5 and plasma6 in region 2, the RCS decreases compared to plasma 1. the RCS increases compared to plasma 4. As shown in Figure 10, the maximum electric field

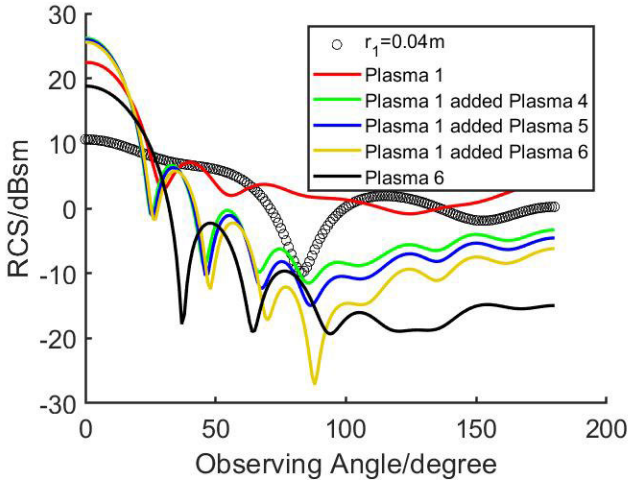

FIGURE 9. Bistatic RCS of the Conducting Sphere with plasma 1 added plasma 4, plasma 5 and plasma 6 obtained by the new Z-FDTD method.

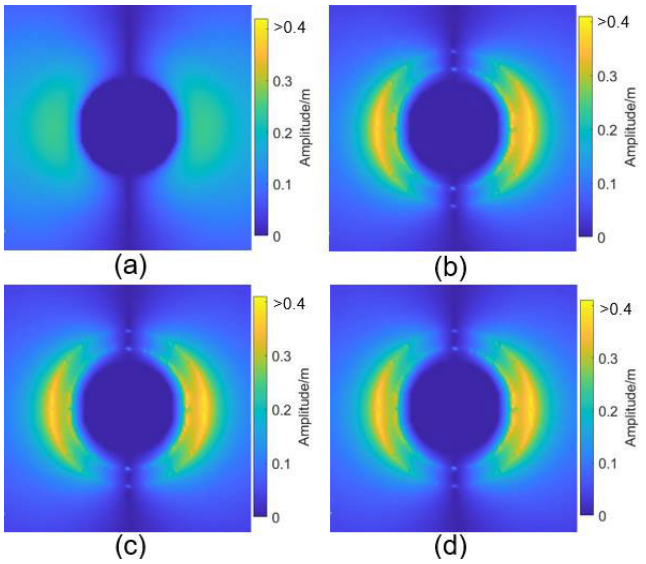

FIGURE 10. (a) Electric field amplitude of conducting sphere, (b) Electric field amplitude of conducting sphere with plasma 1 added plasma 4, (c) Electric field amplitude of conducting sphere with plasma 1 added plasma 5, (d) Electric field amplitude of conducting sphere with plasma 1 added plasma 6.

amplitude is located at the outer edge of each plasma layer region. Compared to Figure 5 (b), the electric field amplitude is enhanced in Region 1, and the zero-value region of the electric field amplitude is reduced.Compared to a uniform plasma, the plasma stealth effect is more pronounced in non-uniform plasma. When the RCS is attenuated, the electric field amplitude increases. When the RCS is enhanced, the zero-value region in the plasma enlarges.

Three assistant variables **D**, **I**, and **S** are used in the traditional method. In the new method, only one auxiliary variable **J** is required. This new method significantly improved the calculation speed.

IV. CONCLUSION

In this paper, a new calculation method for electromagnetic wave propagation in plasma based on the traditional ZT-FDTD method is presented in detail, the calculating formulas is derived, the correctness and the efficacy of this method is proved using several examples. In the traditional ZT-FDTD method, the FDTD numerical method should increase subsidiary variables **D**, **I**, and **S**. With this method, only one subsidiary variable **J** must be added. The numerical results show that this method improves the computational efficiency by **9.8** percent compared to the traditional ZT-FDTD method. The improved ZT-FDTD method has the characteristics of a simple derivation, easy programming, and strong universality. Therefore, this method is worthy of further generalization for the study of dispersive media. In the improved formula, it is easier to see that an increase in the plasma frequency can increase the influence of plasma on the electric field, whereas an increase in the plasma collision frequency can reduce the influence of plasma on the electric

field. By calculating the bistatic RCS of a conductor sphere covering the plasma, it was demonstrated that the plasma frequency and plasma collision frequency have an increasing and decreasing effect on the RCS. As the plasma frequency increased, the scattering was enhanced, and the electric field amplitude in the plasma decreased. As the collision frequency of the plasma increased, the plasma stealth effect became more pronounced and the electric field amplitude in the plasma decreased. The electric field amplitude changed the most at the outer edge of the plasma field.

REFERENCES

[1] J. Xu, B. Bai, C. Dong, Y. Dong, Y. Zhu, and G. Zhao, "Evaluations of plasma stealth effectiveness based on the probability of radar detection," *IEEE Trans. Plasma Sci.*, vol. 45, no. 6, pp. 938–944, Jun. 2017.

[2] J. P. Rybak and R. J. Churchill, "Progress in reentry communications," *IEEE Trans. Aerosp. Electron. Syst.*, vol. AES-7, no. 5, pp. 879–894, Sep. 1971.

[3] R. J. Luebbers, K. S. Kunz, M. Schneider, and F. Hunsberger, "A finite-difference time-domain near zone to far zone transformation (electromagnetic scattering)," *IEEE Trans. Antennas Propag.*, vol. 39, no. 4, pp. 429–433, Apr. 1991.

[4] T. Kashiwa, N. Yoshida, and I. Fukai, "A treatment by the finite-difference time-domain method of the dispersive characteristics associated with orientation polarization," *IEICE Trans.*, vol. 73, no. 8, pp. 1326–1328, 1990.

[5] D. M. Sullivan, "A frequency-dependent FDTD method for biological applications," *IEEE Trans. Microw. Theory Techn.*, vol. 40, no. 3, pp. 532–539, Mar. 1992.

[6] D. F. Kelley and R. J. Luebbers, "Piecewise linear recursive convolution for dispersive media using FDTD," *IEEE Trans. Antennas Propag.*, vol. 44, no. 6, pp. 792–797, Jun. 1996.

[7] Q. Chen, M. Katsurai, and P. H. Aoyagi, "An FDTD formulation for dispersive media using a current density," *IEEE Trans. Antennas Propag.*, vol. 46, no. 11, pp. 1739–1746, Nov. 1998.

[8] Y.-C. Yang, Z.-Y. Wei, M.-H. Fang, G.-Y. Chen, and Z.-X. Zhang, "Analysis for scattering of plasma sheath of aircraft by ZT-FDTD method in three-dimensional space," *Proc. SPIE*, vol. 7651, pp. 789–797, Apr. 2010.

[9] X.-G. Wu, Y. Hu, P. Wang, and L. Nan, "Interaction of Terahertz wave with plasma based on Z-FDTD," *High Power Laser Part. Beams*, vol. 30, no. 4, pp. 70–75, 2018.

[10] Y. Takahashi, R. Nakasato, and N. Oshima, "Analysis of radio frequency blackout for a blunt-body capsule in atmospheric reentry missions," *Aerospace*, vol. 3, no. 1, p. 2, Jan. 2016.

[11] S. Liu, "Research on finite-difference time-domain algorithm for plasmas and its applications," Ph.D. thesis, College Inf. Sci. Technol., Nanjing Univ. Aeronaut. Astronaut., Nanjing, China, 2010.

[12] W.-F. Chen and Y. Chang, "Analysis of the scattering characteristic for the hypersonic flow field of semi-sphere," *J. Aerosp. Power*, vol. 24, no. 3, pp. 552–557, 2009.

[13] S. Liu, N. Yuan, and J. Mo, "A novel FDTD formulation for dispersive media," *IEEE Microw. Wireless Compon. Lett.*, vol. 13, no. 5, pp. 187–189, May 2003.

[14] J. Chen and J.-G. Wang, "Three-dimensional dispersive hybrid implicit-explicit finite-difference time-domain method for simulations of graphene," *Comput. Phys. Commun.*, vol. 207, pp. 211–216, Oct. 2016.

[15] J. Xu, X. Li, D. Liu, and Y. Wang, "Effects of pulsed magnetic field on density reduction of high flow velocity plasma sheath," *Plasma Sci. Technol.*, vol. 23, no. 7, Jul. 2021, Art. no. 075301.

[16] H. Wang, L. Xu, B. Li, S. Descombes, and S. Lanteri, "An exponential-based DGTD method for modeling 3-D plasma-surrounded hypersonic vehicles," *IEEE Trans. Antennas Propag.*, vol. 68, no. 5, pp. 3847–3858, May 2020.

[17] M. Yan, J. Xu, and X.-W. Yu, "ZT-FDTD analysis of inhomogeneous unmagnetized cylinder," *J. Nav. Univ. Eng.*, vol. 21, no. 3, pp. 18–22, 2009.

[18] A. Scarabosio, J. L. A. Quijano, J. Tobon, M. Righero, G. Giordanengo, D. D'Ambrosio, L. Walpot, and G. Vecchi, "Radiation and scattering of EM waves in large plasmas around objects in hypersonic flight," *IEEE Trans. Antennas Propag.*, vol. 70, no. 6, pp. 4738–4751, Jun. 2022.

[19] Q. Rao, G. Xu, and W. Mao, "Detection of the lunar surface soil permittivity with megahertz electromagnetic wave," *Sensors*, vol. 21, no. 7, p. 2466, Apr. 2021.

[20] S. K. El-Labany, E. K. El-Shewy, H. N. A. El-Razek, and A. A. El-Rahman, "Wave propagation in strongly dispersive superthermal dusty plasma," *Adv. Space Res.*, vol. 59, no. 8, pp. 1962–1968, Apr. 2017.

[21] P. A. Gnoffo, R. N. Gupta, and J. L. Shinn, *Conservation Equations and Physical Models for Hypersonic Air Flows in Thermal and Chemical Nonequilibrium*. Washington, DC, USA: NASA, 1989.

[22] C. L. Britt, "Solution of electromagnetic scattering problems using time domain techniques," *IEEE Trans. Antennas Propag.*, vol. 37, no. 9, pp. 1181–1192, Sep. 1989.

CAIXIONG HAN was born in Ledu, Qinghai, China, in 1993. She received the B.S. degree in electronic information science and technology and the M.S. degree in optics from Xidian University, Xi'an, China, in 2015 and 2018, respectively. Her current research interests include electromagnetic scattering and the finite-difference time-domain method.

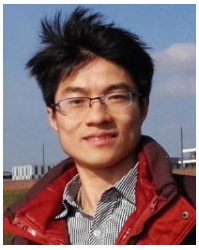

JIAJIE WANG was born in Qianshan, Jiangxi, China, in 1985. He received the B.S. degree in physics from Xidian University, Xi'an, China, in 2006, and the Ph.D. degree in physics from Xidian University, and INSA DE ROUEN, France, in 2011.

From 2016 to 2017, he was a Visiting Scholar with the Leibniz Institute of Material Science, Germany. Since 2012, he has been with Xidian University, where he is currently an Associate Professor. His current research interests include control and applications of laser, research on electromagnetic scattering characteristics of complex targets, and the propagation and scattering characteristics of electromagnetic waves (light waves) in complex random media. He was a recipient of the Optical Society of America (OSA) and the Chinese Institute of Electronics.

LANFANG DING was born in Menyuan, Qinghai, China, in 1984. She received the B.S. degree in physics and the M.S. degree in condensed matter physics from Shaanxi Normal University, Xi'an, China, in 2006 and 2009, respectively. Her current research interests include doping modification of dielectrics and the dielectric properties of microwave ceramics.